Chemical Science

ROYAL SOCIETY OF CHEMISTRY

EDGE ARTICLE

View Article Online
View Journal | View Issue

Cite this: *Chem. Sci.*, 2021, **12**, 11225

All publication charges for this article have been paid for by the Royal Society of Chemistry

Synthesis of a carborane-substituted bis(phosphanido) cobaltate(I), ligand substitution, and unusual P_4 fragmentation†

Peter Coburger, ‡[ab] Julia Leitl,[a] Daniel J. Scott, [a] Gabriele Hierlmeier, [a] Ilya G. Shenderovich, [c] Evamarie Hey-Hawkins *[b] and Robert Wolf *[a]

Received 31st May 2021
Accepted 7th July 2021

DOI: 10.1039/d1sc02948g

rsc.li/chemical-science

Oxidative addition of the P–P single bond of an *ortho*-carborane-derived 1,2-diphosphetane (1,2-$C_2(PMes)_2B_{10}H_{10}$) (Mes = 2,4,6-$Me_3C_6H_2$) to cobalt(−I) and nickel(0) sources affords the first heteroleptic complexes of a carborane-bridged bis(phosphanido) ligand. The complexes also incorporate labile ligands suitable for further functionalisation. Thus, the cobalt(I) complex [K([18]crown-6)][Co{1,2-$(PMes)_2C_2B_{10}H_{10}$}(cod)] (cod = 1,5-cyclooctadiene) bearing a labile cyclooctadiene ligand undergoes facile ligand exchange reactions with isonitriles and *tert*-butyl phosphaalkyne with retention of the bis(phosphanido) ligand. However, in the reaction with one equivalent of P_4, the electron-rich bis(phosphanido) moiety abstracts a single phosphorus atom with formation of a new P_3 chain, while the remaining three P atoms derived from P_4 form an η^3-coordinating *cyclo*-P_3 ligand. In contrast, when the same reaction is performed with two equivalents of the cobalt(I) complex, a dinuclear product is formed which features an unusual P_4 chain in its molecular structure.

Introduction

Terminal phosphanides, PR_2^-, are remarkable ligands for transition metal coordination chemistry due to their flexible and unusual reaction behaviour. Even when acting as simple 'spectator' ligands, their properties as very strong σ and π donors can dramatically influence the electronic structure and hence the reactivity at the metal.[1] In addition, the presence of sterically and electronically accessible lone pairs of electrons leads to highly reactive metal–phosphorus bonds,[2–19] allowing for additional, 'non-innocent' reactivity toward substrates including Brønsted acids,[4,10–12,17] electrophiles,[4,7,10,17] and unsaturated π systems.[19] Moreover, terminal phosphanido complexes can serve as metalloligands for heterobimetallic complexes.[5,7,10] These exciting properties make transition metal phosphanido complexes attractive targets for study, and they have been exploited for a number of applications including palladium-catalysed Suzuki cross-couplings, where bimetallic phosphanido complexes of ruthenium and palladium show excellent catalytic performance.[2,3] Terminal phosphanido complexes have also been utilised in catalytic hydrophosphination and dehydrocoupling reactions.[6,8,11,13,16]

While monodentate phosphanido ligands have been quite extensively explored, complexes with chelating, terminal bis(phosphanido) ligands are comparably understudied. In addition to the improved stability and rigidity that are inherent to the use of chelates, such ligands are expected to lead to further enhancements in reactivity due to the presence of two non-innocent nucleophilic sites in close proximity, as well as the cumulative electronic effects of the two donor moieties on the transition metal centre. Pertinent examples of 3d metal complexes of such species are shown in Fig. 1.[20–24] They have been synthesised in three different ways: (a) salt metathesis of alkali metal bis(phosphanides) (**I** and **II**),[20,22] (b) oxidative addition of a P–P bond to a transition metal centre (**III** and **IV**),[21,23] and (c) elimination of phenyl groups from precursor diphenylphosphinoarene ligands (**V**).[24]

In our own contribution to this area, we recently reported the synthesis of anionic cobalt(III) complex **IV** by reaction of an *ortho*-carborane-based diphosphetane with the anionic cobalt(−I) complex $[Co(cod)_2]^-$ (cod = 1,5-cyclooctadiene).[23] Oxidative addition of the P–P single bonds from two equivalents of the diphosphetane to the cobalt(−I) centre affords two bis(phosphanido) moieties, which coordinate as chelate ligands at a single cobalt atom. Remarkably, the strong σ and π donation of the P donor atoms results in a low-spin (singlet) electronic ground state despite the (pseudo)tetrahedral coordination geometry.

[a]*Institute of Inorganic Chemistry, Universität Regensburg, 93040 Regensburg, Germany. E-mail: Robert.Wolf@chemie.uni-regensburg.de*

[b]*Institute of Inorganic Chemistry, Universität Leipzig, Johannisallee 29, 04103 Leipzig, Germany. E-mail: hey@uni-leipzig.de; Web: https://anorganik.chemie.uni-leipzig.de/anorganik/ak-hey-hawkins/*

[c]*Institute of Organic Chemistry, Universität Regensburg, 93040 Regensburg, Germany*

† Electronic supplementary information (ESI) available: Experimental procedures, detailed spectral and crystallographic characterisation, DFT calculations, electrochemical data, catalysis plots. See DOI: 10.1039/d1sc02948g

‡ Present address: Dr. P. Coburger, Laboratory of Inorganic Chemistry, ETH Zürich, Vladimir-Prelog-Weg 1-5/10, CH-8093 Zürich, Switzerland.

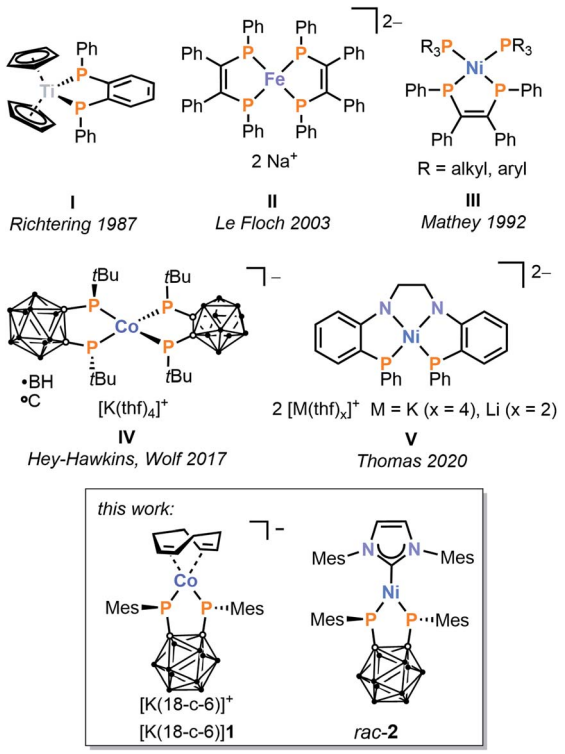

Fig. 1 Examples of first-row transition metal complexes with chelating terminal bis(phosphanido) ligands.

Although this is an impressive demonstration of the powerful effect of the carborane-bridged bis(phosphanido) ligand, the further reactivity of the coordinatively saturated, heteroleptic complex **IV** is unfortunately limited. We therefore sought to test the generality of our synthetic approach to obtain new, low-valent 3d metal complexes, and particularly *heteroleptic* examples that retain vacant coordination sites and/or labile ligands suitable for further functionalisation.

Reported herein are the results of this investigation, including the preparation of complexes of Co ([*rac*-**1**]$^-$) and Ni (*rac*-**2**), each incorporating a single bis(phosphanido) moiety alongside potentially labile ligands. While the insolubility and instability of the nickel compound **2** precluded follow-up chemistry, further studies have revealed a versatile reactivity of the cobalt complex [K(18-c-6)(thf)][*rac*-**1**] (18-c-6 = [18]crown-6) toward various substrates, resulting in a range of derivatives ([*rac*-**6**]$^-$ to [*rac*-**9**]$^{2-}$), which have been structurally and spectroscopically characterised. These include a remarkable complex ([*meso*-**8**]$^-$) incorporating both *cyclo*-P_3 and carborane-bridged triphospholanide ligands, resulting from a well-behaved fragmentation of white phosphorus (P_4).

Results and discussion

Synthesis of heteroleptic complexes [K(18-c-6)(thf)][*rac*-1] and *rac*-2

Previously we found that reactions of a *tert*-butyl-substituted *ortho*-carborane-based diphosphetane with the cobalt(−I) sources $[Co(cod)_2]^-$ and $[Co(anthracene)_2]^-$ in a 2 : 1 stoichiometric ratio afford the homoleptic complex **IV** shown in Fig. 1, which features two bis(phosphanido) ligands.[23]

When the same reaction is performed in a 1 : 1 stoichiometric ratio, complex **IV** is again observed as the only product by $^{31}P\{^1H\}$ NMR spectroscopy, while formation of a heteroleptic 1 : 1 complex with one bis(phosphanido) ligand coordinating at cobalt(I) was not detectable. In light of these results and anticipating that the desired monoligation should be favoured by an increase in steric bulk, attention was therefore shifted to preparation of a larger, mesityl-substituted diphosphetane, which was achieved *via* the two-step reaction sequence shown in Scheme 1. This synthetic route was adapted from the preparation of the original *tert*-butyl-substituted diphosphetane.[25] Deprotonation of the parent *ortho*-carborane **3** using *n*BuLi and subsequent *in situ* treatment of the product with dibromo(mesityl)phosphane[26] affords the brominated bis(phosphane) **4** as a mixture of stereoisomers.[27] Direct treatment of this crude material with potassium graphite (two equivalents) in diethyl ether straightforwardly affords diphosphetane *rac*-**5** in modest overall yield.§ The proposed diphosphetane structure in *rac*-**5** was confirmed by multinuclear NMR spectroscopy and elemental analysis (see the ESI†).

With the desired precursor *rac*-**5** in hand, attention was shifted to the preparation of the target metal complexes. Gratifyingly, treatment of *rac*-**5** with $[K(thf)_{0.2}][Co(cod)_2]$ in a diethyl ether/*n*-hexane mixture (2 : 5 v/v) cleanly affords a single reaction product, exhibiting a singlet in the $^{31}P\{^1H\}$ NMR spectrum at 101.3 ppm. This chemical shift is upfield compared to that observed for **IV** (201.8 ppm in THF-d_8), suggesting that it does not correspond to a homoleptic 2 : 1 complex. Addition of [18]crown-6 to the crude reaction mixture affords the crown ether adduct [K(18-c-6)(thf)][*rac*-**1**]. This species can be isolated as dark orange crystals in good yield (67%) by crystallisation from THF/*n*-hexane (Scheme 2). The formulation of the anion [*rac*-**1**]$^-$ as $[Co\{1,2\text{-}(PMes)_2C_2B_{10}H_{10}\}(\text{-cod})]^-$ is supported by elemental analysis as well as multinuclear NMR spectroscopy. The ^1H NMR spectrum in THF-d_8 shows a single set of mesityl resonances and also demonstrates the presence of a coordinated cod ligand, with olefinic protons that are significantly shielded compared to the free ligand (2.93 ppm *vs.* 5.58 ppm) as a result of metal–ligand π backbonding. This chemical shift is similar to that observed in $[K(thf)_2][Co(BIAN)(\text{-cod})]$ (BIAN = 1,2-bis(2,6-diisopropylphenylimino)acenaphthene) (2.91 ppm).[28] Two broad resonances are observed in the $^{11}B\{^1H\}$ NMR spectrum at −9.4 and −7.9 ppm, consistent with previous observations of the carborane-bridged bis(phosphanido) ligand in

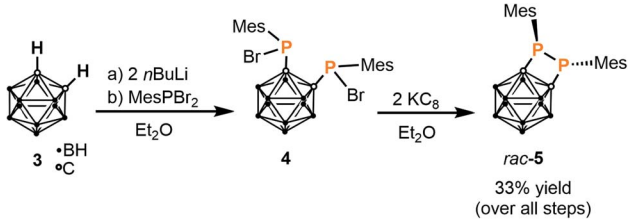

Scheme 1 Synthesis of mesityl-substituted diphosphetane *rac*-**5**.

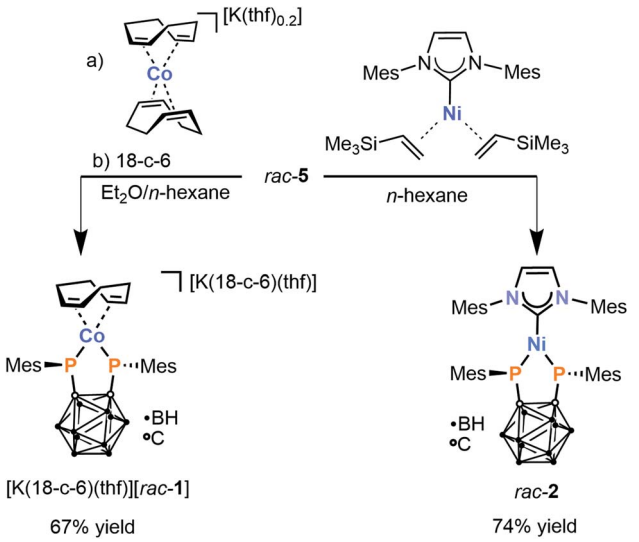

Scheme 2 Synthesis of heteroleptic 3d metal complexes [K(18-c-6)(thf)][*rac*-**1**] and *rac*-**2** *via* oxidative addition of diphosphetane *rac*-**5** (18-c-6 = [18]crown-6).

IV,[23,29] while the carborane carbon atoms are detected at *ca.* 92 ppm in the $^{13}C\{^1H\}$ NMR spectrum.

The singlet in the $^{31}P\{^1H\}$ NMR spectrum of [K(18-c-6)][*rac*-**1**] is significantly broadened (ν_{FWHM} = 140 Hz), consistent with quadrupolar relaxation induced by the ^{59}Co nucleus (100% natural abundance, I = 7/2). Further, conclusive proof of the structure of the anion [*rac*-**1**]$^-$ was obtained by X-ray crystallographic analysis of single crystals of the salt [K(dme)$_4$][*rac*-**1**] (dme = 1,2-dimethoxyethane; *vide infra*).

Having succeeded in the isolation of the desired heteroleptic Co complex, an analogous Ni complex was also targeted. Indeed, a comparable reaction of diphosphetane *rac*-**5** with the nickel(0) source [Ni(IMes)(η^2-H$_2$C=CHSiMe$_3$)$_2$] (IMes = 1,3-bis(2,4,6-trimethylphenyl)imidazolin-2-ylidene) in *n*-hexane furnished a single product *rac*-**2** in good isolated yield (74%, Scheme 2).

Purple, crystalline *rac*-**2** is poorly soluble in hydrocarbons and aromatic solvents. In polar solvents such as THF it is slightly soluble, but decomposes over the course of several minutes, as is evident from a colour change from purple to light yellow and the observation of several new, unidentified resonances in the $^{31}P\{^1H\}$ NMR spectrum (see the ESI† for details). While this prevented characterisation by conventional solution-phase NMR spectroscopy, *rac*-**2** can nevertheless confidently be formulated as the neutral complex [Ni{1,2-(PMes)$_2$C$_2$B$_{10}$H$_{10}$}(IMes)] – the first example of a Ni complex incorporating a carborane-substituted bis(phosphanido) ligand – on the basis of elemental analysis, X-ray crystallography (*vide infra*), and solid-state $^{31}P\{^1H\}$ MAS NMR spectroscopy (see the ESI, Fig. S9†). Line fitting of the NMR spectrum reveals the three components of the chemical shift tensor in *rac*-**2**, δ_{11} = 424 ppm; δ_{22} = 33 ppm; δ_{33} = −67 ppm. This corresponds to an isotropic ^{31}P NMR shift of 130 ppm, which is similar to the chemical shift of complex [K(18-c-6)(thf)][*rac*-**1**] (δ = 100.3 ppm) observed in solution.

Reactivity studies of complex [K(18-c-6)(thf)][*rac*-1]

While attempts to study the reactivity of Ni complex *rac*-**2** have been hampered by its limited solubility and stability in common solvents, the Co complex [K(18-c-6)(thf)] [*rac*-**1**] is fully amenable to further investigation. Crucially, the anion [*rac*-**1**]$^-$ features a potentially labile 1,5-cyclooctadiene ligand, which could provide a valuable handle for further reactivity and thus allow the targeted synthesis of new and more elaborate bis(phosphanido) complexes.

In order to demonstrate this potential for ligand substitution, we began by examining the reaction of [K(18-c-6)(thf)][*rac*-**1**] with two equivalents of cyclohexyl isonitrile (CyNC) as shown in Scheme 3. Satisfyingly, this reaction cleanly affords the 16 VE isonitrile complex [K(18-c-6)(dme)][Co{1,2-(PMes)$_2$C$_2$B$_{10}$H$_{10}$}(CyNC)$_2$] ([K(18-c-6)(dme)][*rac*-**6**]), which can be isolated as red crystals in good yield (55%) after work-up and recrystallisation from dme/*n*-hexane. Like its precursor [K(18-c-6)(thf)][*rac*-**1**], the composition and structure of the product [K(18-c-6)(dme)][*rac*-**6**] could be confirmed by elemental analysis, multinuclear NMR spectroscopy (which shows comparable resonances for the bis(phosphanido) ligand, alongside those expected for the CyNC moieties), and X-ray crystallography (*vide infra*). The presence of the CyNC ligands was further confirmed by the IR spectrum of solid [K(18-c-6)(dme)][*rac*-**6**], which shows two strong CN vibrations at 2029 and 1938 cm^{-1}. In comparison, the free isonitrile shows a CN stretching vibration at 2136 cm^{-1}. The substantial changes of the CN stretching frequency of 198 cm^{-1} in case of the most intense vibration suggests that the bis(phosphanido) ligand in [*rac*-**6**]$^-$ acts as an exceptional σ-donor.¶ In fact, the observed CN stretching frequencies are considerably lower than typically found in mixed cobalt(I)-isonitrile complexes with phosphane ligands.[30–32] However, in those complexes the cobalt atom is usually coordinated by three to four isonitrile ligands which hampers the comparability to [K(18-c-6)(dme)][*rac*-**6**].

As the simple ligand substitution reaction between [K(18-c-6)(thf)][*rac*-**1**] and CyNC was successful, more elaborate transformations were pursued. We have previously highlighted how the dimerisation of phosphaalkynes in the coordination sphere of low-valent Co complexes can be used to access coordinatively and chemically versatile complexes of 1,3-diphosphabutadienes.[33–35]

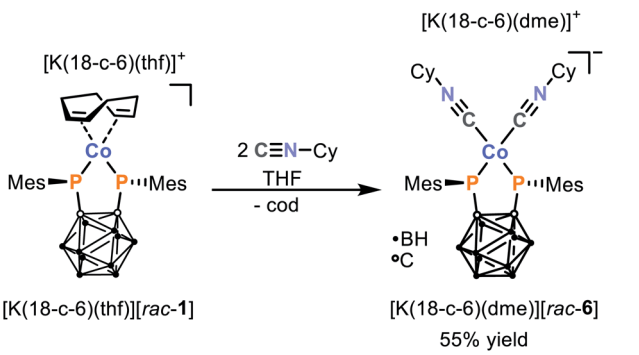

Scheme 3 Synthesis of isonitrile complex [K(18-c-6)(dme)][*rac*-**6**] *via* ligand exchange of [K(18-c-6)(thf)][*rac*-**1**] (18-c-6 = [18]crown-6).

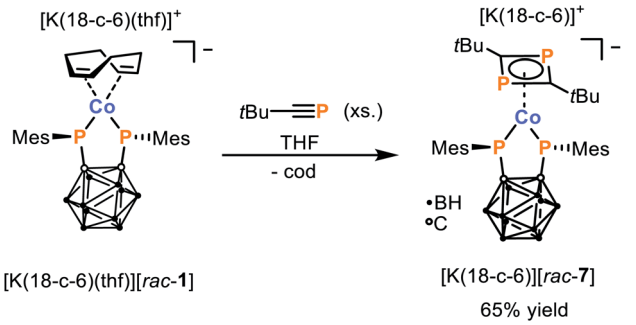

Scheme 4 Synthesis of 1,3-diphosphabutadiene complex [K(18-c-6)][*rac*-**7**] *via* reaction of *t*BuCP with [K(18-c-6)(thf)][*rac*-**1**].

Thus, the reaction between [K(18-c-6)(thf)][*rac*-**1**] and *tert*-butyl phosphaalkyne, *t*BuCP, was investigated. As hoped, this leads to the clean and exclusive formation of the 16 VE complex [K(18-c-6)][$Co(\eta^4$-1,3-$tBu_2C_2P_2)\{1,2$-$(PMes)_2C_2B_{10}H_{10}\}$] ([K(18-c-6)][*rac*-**7**]) which can be isolated in 65% yield after washing of the crude product with diethyl ether (Scheme 4). The complex anion [*rac*-**7**]$^-$ contains both the chelating bis(phosphanido) ligand and an η^4-coordinating 1,3-diphosphacyclobutadiene ($tBu_2C_2P_2$) ligand, as was confirmed by a combination of elemental analysis, NMR spectroscopy, and X-ray crystallography.

Finally, we also studied the reactivity of [K(18-c-6)(thf)][*rac*-**1**] toward white phosphorus (P_4). The reactivity of P_4 toward transition metal complexes has been a topic of intense interest in recent years due to a strong desire to discover alternatives to the wasteful and indirect methods currently used to transform P_4 industrially.[36–38] Notably, while this allotrope is well known for its high reactivity, the development of selective reactions of P_4 is typically very challenging. Nevertheless, the 1 : 1 reaction between [K(18-c-6)(thf)][*rac*-**1**] and P_4 results in formation of a single major product, namely the 18 VE cobalt(I) complex [K(18-c-6)][*meso*-**8**], which can be isolated from the reaction mixture in 49% yield (Scheme 5).‖

Based on the reactivity of [K(18-c-6)(thf)][*rac*-**1**] toward CyNC and *t*BuCP, it had been anticipated that the reaction with P_4 would most likely lead to substitution of cod by a *cyclo*-P_4 ligand, as has been observed in previous reactions of P_4 with complexes of the type $[L_2Co(cod)]^-$ (L_2 = chelating bidentate ligand).[28,39] Instead, X-ray crystallographic analysis (*vide infra*) revealed the unexpected fragmentation of P_4 shown in Scheme 5. The anion [*meso*-**8**]$^-$ represents a rare anionic *cyclo*-P_3 cobalt complex, the only other reported examples are [nBu$_4$N][(PHDI)$Co(\eta^3$-$P_3)$(CN)] (PHDI = bis(2,6-diisopropylphenyl) phenanthrene-9,10-diimine), [Cat][Cp‴$Co(\eta^3$-$P_3)$] ([Cat] = $[K(thf)_{0.7}]^+$ and $[(TMC)_2P]^+$, TMC = 1,3,4,5-tetramethylimidazolin-2-ylidene, Cp‴ = 1,2,4-tri-*tert*-butyl-cyclopentadienide).[39–41] Furthermore, instead of the expected dianionic bis(phosphanido) ligand, [*meso*-**8**]$^-$ features a monoanionic triphospholanido ligand, in an unprecedented η^3-coordination mode.

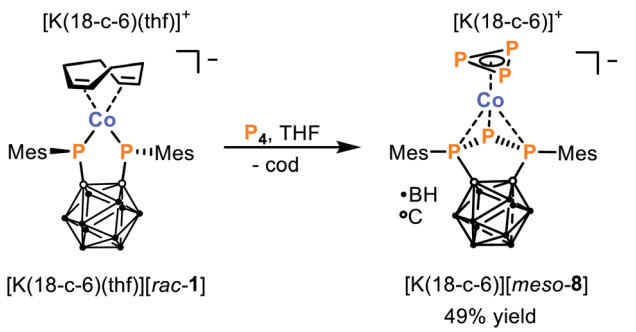

Scheme 5 Fragmentation of P_4 *via* reaction with [K(18-c-6)(thf)][*rac*-**1**] to generate [K(18-c-6)][*meso*-**8**].

Elemental analysis and NMR spectroscopic investigations are both consistent with the structure revealed crystallographically. The $^{11}B\{^1H\}$ NMR spectrum of [K(18-c-6)][*meso*-**8**] shows a similar pattern to those previously reported for *ortho*-carborane-substituted triphospholanes, with three broad resonances centred at −12.5, −8.6 and −2.3 ppm.[42,43] The presence of the mesityl substituents is evidenced by singlets in the ^1H NMR spectrum for the *ortho*-methyl groups (2.80 and 2.82 ppm), *para*-methyl groups (2.24 ppm), and aromatic hydrogen atoms (6.83 and 6.87 ppm), with the number of resonances indicating hindered rotation about the P–C_{aryl} bond. The $^{31}P\{^1H\}$ NMR spectrum is likewise in agreement with the solid-state molecular structure, showing a doublet at 30.0 ppm and triplet at −250.7 ppm ($^1J_{PP}$ = 325 Hz) for the triphospholanido ligand, and a characteristically upfield singlet for the *cyclo*-P_3^- ligand at −250.9 ppm.[39,40]

The structure of [*meso*-**8**]$^-$, and its divergence from those observed previously for products derived from related $[L_2Co(cod)]^-$, again highlights the non-innocence and dramatic impact of the bis(phosphanido) ligand on the reactivity. Overall, it can be seen that the P_4 molecule is formally split into P_3^- and P^+ moieties, which are ultimately bound to the metal centre and bis(phosphanido) ligand, respectively. Intuitively, it seems likely that this fragmentation would proceed *via* initial coordination of P_4 to the complex anion [*rac*-**1**]$^-$, followed by intramolecular abstraction of a P^+ fragment by the nucleophilic phosphanido moieties. Related transition-metal mediated [3 + 1] fragmentations of P_4 have rarely been reported in the literature.[40,44–46] To the best of our knowledge, our system is the first which incorporates both the resulting P_3 and P_1 fragment in the same product.

To provide deeper insight, a combined DFT and DLPNO-CCSD(T) study was conducted (see the ESI† for details), and the calculated mechanism is shown in Fig. 2. In the first step, the cod ligand of [*rac*-**1**]$^-$ is replaced with P_4, leading to the formation of complex **Int1** which contains a *side-on* coordinated P_4 moiety where one P–P bond is significantly weakened (2.740 Å). In the next step – which is slightly exothermic with respect to **Int1** (ΔE = −3.8 kcal mol^{-1}) – removal of a P^+ atom from the P_4 moiety is achieved through attack by a single phosphanido moiety. This step proceeds *via* transition state **TS1** to produce a second intermediate **Int2** containing the thus formed P_3^- ligand, with the abstracted P atom bridging one of the original Co–P bonds.

In the final, rate-determining step, interaction of this P atom with the second phosphanido moiety results in formation of the

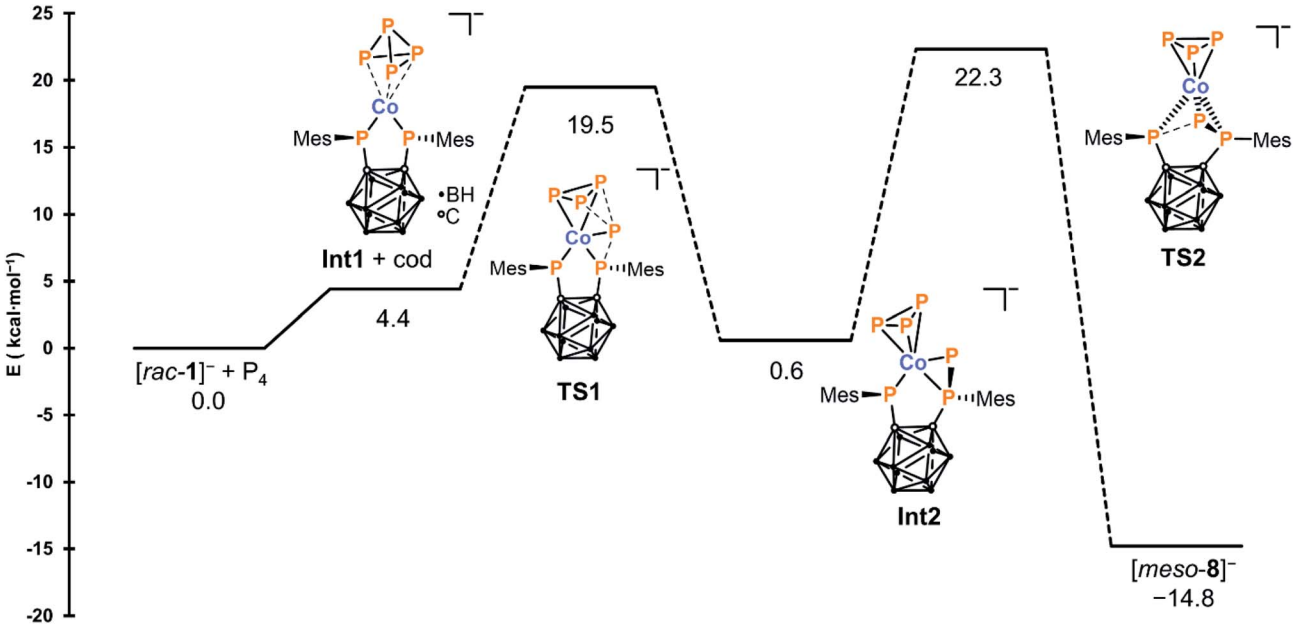

Fig. 2 Calculated mechanism for the formation of [*meso*-**8**]$^-$ from [*rac*-**1**]$^-$ and P_4. Energies were obtained at the DLPNO-CCSD(T)/CBS level.

triphospholanido moiety, forming the final product *rac*-**8**$^-$ *via* transition state **TS2** with a total activation barrier of 22.3 kcal mol^{-1}. In the calculated mechanism, all activation barriers are easily accessible at 298 K and none of the intermediates is a thermodynamic sink. This is in agreement with reaction monitoring by $^{31}P\{^1H\}$ NMR spectroscopy, where only the direct formation of [*meso*-**8**]$^-$ without intermediates is observed (see the ESI, Fig. S26†).

In the above reaction, the complex [K(18-c-6)][*meso*-**8**] is consistently isolated containing *ca.* 5 to 10% of a minor impurity. This side product can be synthesised cleanly and deliberately by treating an *in situ* prepared solution of [*rac*-**1**]$^-$ in THF with just half an equivalent of P_4, and subsequent addition of [18]crown-6. Washing of the crude product with diethyl ether affords the homobimetallic complex [K(18-c-6)]$_2$[*rac*-**9**] as a purple solid in 21% yield (Scheme 6). X-ray crystallographic analysis (*vide infra*) revealed the structure of the complex dianion [*rac*-**9**]$^{2-}$, which features a bridging, open-chain μ-η^4:η^4-P_4^{2-} ligand that can be described as a *cis*-1,3-tetraphosphabutadienediide. Complexes of this ligand are extremely scarce, and to the best of our knowledge only three other examples are known, namely [K(dme)$_4$][{(BIAN)Co}$_2$(μ-η^4:η^4-P_4)], [{Cp″Fe}$_2$(μ-η^4:η^4-P_4)] (Cp″ = 1,3-di-*tert*-butyl-cyclopentadienide) and [{Cp‴Fe}$_2$(μ-η^4:η^4-P_4)].[28,47,48]

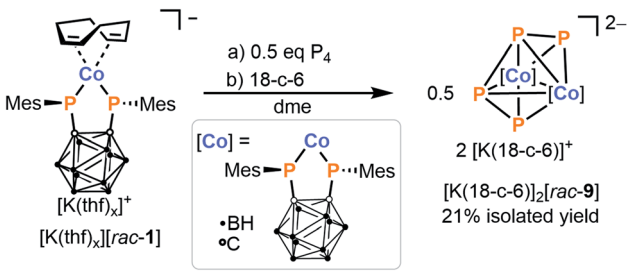

Scheme 6 Synthesis of homodinuclear complex [K(18-c-6)]$_2$[*rac*-**9**] *via* reaction of P_4 with 2 equivalents of [K(thf)$_x$][*rac*-**1**].

The $^{11}B\{^1H\}$ NMR spectrum of [K(18-c-6)]$_2$[*rac*-**9**] shows a single broad resonance at −7.1 ppm for the carborane ligand backbone, while the ^1H NMR spectrum shows the expected *ortho*-Me, *para*-Me and aromatic resonances for the inequivalent mesityl groups. At 298 K, the $^{31}P\{^1H\}$ NMR spectrum in THF-d$_8$ solution consists of three broad resonances corresponding to the P_4^{2-} ligand (P3: 423.6 ppm, P4, P5: −42.0 ppm, P6: 223.1 ppm; *vide infra* for detailed structural discussion, atom labels according to Fig. 3) and two singlets (P1: 58.0 ppm, P2: 119.2 ppm) corresponding to the two chemically inequivalent phosphorus nuclei within each bis(phosphanido) ligand. These assignments have been made by reference to DFT-calculated ^{31}P NMR shifts in [*rac*-**9**]$^{2-}$ (*vide infra*). The number of signals excludes the presence of a fast fluxional process that would render the atoms of the P_4^{2-} chain equivalent on the NMR timescale at room temperature, in contrast to the iron complexes [{Cp″Fe}$_2$(μ-η^4:η^4-P_4)] and [{Cp‴Fe}$_2$(μ-η^4:η^4-P_4)] (for each of which only one singlet was observed at 165 ppm and 91.0 ppm, respectively). Nevertheless, variable-temperature NMR studies do suggest some limited fluxionality, and at 233 K the resonances of the P_4^{2-} moiety are split further, with four distinct signals (P3: 418.8 ppm, P4: −49.1, P5: −42.3 ppm, P6: 216.5 ppm) and resolved $^1J_{PP}$ couplings ($^1J_{P3-P4}$ = 379 Hz, $^1J_{P4-P5}$ = 217 Hz, $^1J_{P5-P6}$ = 478 Hz).

Time-resolved $^{31}P\{^1H\}$ NMR spectroscopic monitoring confirmed that formation of [*rac*-**9**]$^{2-}$ occurs *via* the reaction of [*meso*-**8**]$^-$ with a second equivalent of cobaltate [*rac*-**1**]$^-$. Interestingly, when pre-formed [K(18-c-6)][*rac*-**1**] is used instead of *in situ* generated, crown ether-free [*rac*-**1**]$^-$, the reaction proceeds considerably more slowly, indicating that the potassium counterion might play a significant role in facilitating the formation of [*rac*-**9**]$^{2-}$ (see the ESI, Fig. S27†).

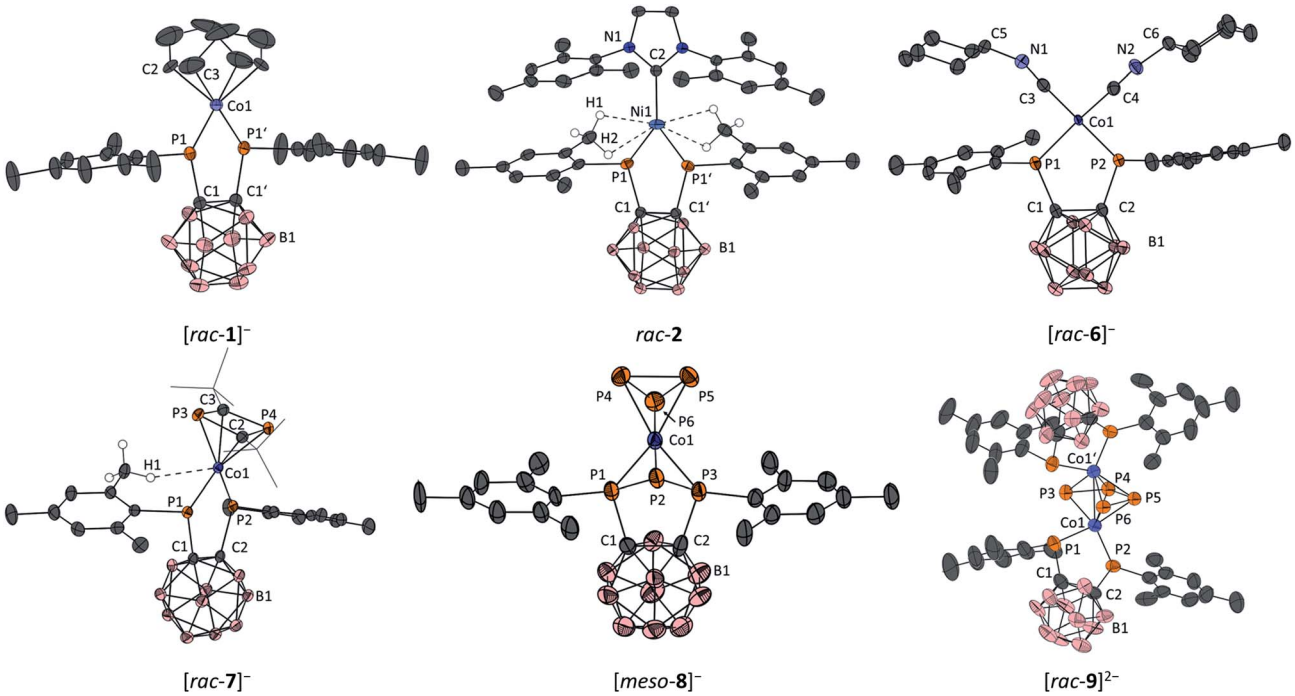

Fig. 3 Molecular structures of [K(dme)$_4$][*rac*-**1**] (top left), *rac*-**2** (top centre), [K(18-c-6)(dme)][*rac*-**6**] (top right), [K(dme)$_4$][*rac*-**7**] (bottom left), [K(18-c-6)(dme)$_2$][*meso*-**8**] (bottom centre) and [K(dme)][K(dme)$_2$][*rac*-**9**] (bottom right) with ellipsoids at the 50% probability level. Only the anions are shown; the counterions are omitted for clarity. For all compounds, hydrogen atoms, except those interacting with Co1 in [*rac*-**7**]$^-$ and with Ni1 in **2**, are omitted for clarity. Additionally, the *tert*-butyl groups in **7**$^-$ are drawn as wireframes for clarity. For [*rac*-**9**]$^{2-}$, only one of two crystallographically independent anions in the asymmetric unit is shown; structural parameters of the second molecule are given in the ESI.† Symmetry-generated atoms are marked with a prime symbol (′). Selected bond lengths [Å] and angles [°] of [K(dme)$_4$][*rac*-**1**]: C1–C1′ 1.657(5), Co1–P1 2.1857(8), Co1–C2 2.041(7), Co1–C3 2.073(6), C2–C3 1.343(9), P1–Co1–P1′ 88.84(2), $\sum_{P1}$ 339.8(3) (sum of bond angles around P1); *rac*-**2**: C1–C1′ 1.650(2), Ni1–P1 2.1264(4), Ni1–C2 2.041(7), Co1–C3 1.962(2), Ni1–H1 2.56, Ni1–H2 2.88, P1–Ni1–P1′ 91.35(1), $\sum_{P1}$ 323.2(2). [K(18-c-6)(dme)][*rac*-**6**]: C1–C2 1.669(2), Co1–P1 2.1874(6), Co1–P2 2.1570(6), Co1–C3 1.784(2), Co1–C4 1.784(2), C3–N1 1.183(2), C4–N2 1.174(3), P1–Co1–P2 91.47(2), C3–N1–C5 153.6(2), C4–N2–C6 153.3(2), $\sum_{P1}$ 328.5(2), $\sum_{P2}$ 337.8(2); [K(dme)$_4$][*rac*-**7**]: C1–C2 1.672(2), Co1–P1 2.2371(4), Co1–P2 2.0871(5), Co1–C2 2.049(2), Co1–C3 2.099(1), Co1–P3 2.2750(5), Co1–P4 2.2454(5), Co1–H1 2.64, C2–P3 1.800(1), C2–P4 1.805(2), P1–Co1–P2 92.29(2), $\sum_{P1}$ 325.3(2), $\sum_{P2}$ 351.1(2); [K(18-c-6)(dme)$_2$][*meso*-**8**]: C1–C2 1.65(1), Co1–P1 2.136(2), Co1–P2 2.382(2), Co1–P3 2.141(2), Co1–P4 2.283(4), Co1–P5 2.276(2), Co1–P6 2.267(2), P1–P2 2.175(3), P4–P5 2.142(3), P5–P6 2.164(3), P1–P2–P3 78.0(1); [K(dme)$_x$]$_2$[*rac*-**9**]: C1–C2 1.685(9), Co1–P1 2.246(2), Co1–P2 2.170(2), Co1–P3 2.293(2), Co1–P4 2.333(2), Co1–P5 2.340(2), Co1–P6 2.183(2), Co1–Co1′ 2.651(1), P3–P4 2.095(3), P4–P5 2.336(3), P5–P6 2.112(3), P1–Co1–P2 92.63(7), $\sum_{P1}$ 323.5(8), $\sum_{P2}$ 340.7(7).

Structural characterisation of *rac*-2 and complex anions [*rac*-1]$^-$, [*rac*-6]$^-$, [*rac*-7]$^-$, [*meso*-8]$^-$ and [*rac*-9]$^{2-}$

Crystals suitable for X-ray diffraction experiments could be obtained for all complexes described in the present study (see Fig. 3 for depictions and selected bond lengths and angles). Three complexes ([*rac*-**1**]$^-$, [*rac*-**7**]$^-$ and [*rac*-**9**]$^{2-}$) were crystallised from dme solutions without any 18-c-6 ligand. Of these, [*rac*-**1**]$^-$ and [*rac*-**7**]$^-$ were crystallised with the [K(dme)$_4$]$^+$ counterion. In the case of [*rac*-**9**]$^{2-}$, two molecules of the complex dianion were contained in the asymmetric unit. Due to severe disorder and the low quality of the crystals, only the counterions [K(dme)$_n$]$^+$ (n = 1, 2) coordinating to one of the dianions in the asymmetric unit could be modelled properly. The counterions of the second dianion were removed from the unit cell using the SQUEEZE procedure of the PLATON program package,[49] and the obtained bond lengths and angles should therefore be analysed with care. Nevertheless, the identity of [*rac*-**9**]$^{2-}$ can be unambiguously derived from the X-ray data. The other complexes were obtained as [K(18-c-6)(dme)]$^+$ ([*rac*-**6**]$^-$) or [K(18-c-6)(dme)$_2$]$^+$ ([*meso*-**8**]$^-$) salts. Also, the anions [*rac*-**1**]$^-$, [*rac*-**6**]$^-$ and [*rac*-**9**]$^{2-}$ are located on symmetry elements in the solid state.

In all complexes, the C–C bond within the *ortho*-carborane backbone is in the typical range for carborane-substituted bis(phosphane) complexes.[27,50] In the case of the complex anions [*rac*-**1**]$^-$, [*rac*-**6**]$^-$ and [*rac*-**9**]$^{2-}$, the Co–P bonds formed by the bis(phosphanido) ligand are in the range of single bonds,[51–59] and significantly elongated compared to **IV** (2.1437(5) Å), consistent with the lower oxidation state of the metal (*vide infra*). For these complexes, the sums of bond angles around the phosphorus atoms range from 328.5(2)° ([*rac*-**6**]$^-$) to 340.7(7)° ([*rac*-**9**]$^{2-}$), showing significant pyramidalisation. Thus, these structural data suggest the presence of a dominant σ–donor interaction between the phosphanido moieties and the cobalt centres, with limited contributions from P=Co π bonding. This is confirmed by quantum chemical calculations (*vide infra*).

For [*rac*-**1**]$^-$, a distorted square-planar environment is observed ($\tau_4 = 0.22$, where a value of 0 corresponds to an ideal square-planar structure, while a value of 1 indicates a perfectly tetrahedral structure).[60] The η^4-coordinating cod ligand shows similar structural parameters to those found in the related cobalt(I) complex [K(thf)$_2$][Co(BIAN)(cod)].[28]

In *rac*-**2**, the nickel atom adopts a perfectly trigonal planar environment (sum of bond angles around Ni: 360.00(2)°), and the Ni1–P1 bond (2.1264(4) Å) is shorter than observed for the related bis(phosphanido) nickel complex **II** (Ni–P 2.164(1) and 2.173(1) Å, Fig. 1). Despite this, the sums of bond angles around the phosphorus atoms in *rac*-**2** (323.2(2)°) still indicate trigonal pyramidal geometries, which suggests that the bis(phosphanido) ligand again acts mainly as a σ donor. Another notable feature of the structure is a collection of short contacts between the nickel centre and several hydrogen atoms of the closest methyl groups of the mesityl substituents in the bis(phosphanido) ligand. The observed Ni···H distances range from 2.56 to 2.88 Å; such values indicate anagostic interactions, which are likely attributable to the comparatively low coordination number of the nickel atom.[61]

The solid state molecular structure of anion [*rac*-**6**]$^-$ confirms the substitution of cod by two isonitrile ligands. The cobalt atom adopts a highly distorted square planar environment close to a seesaw geometry ($\tau_4 = 0.37$). The two Co–P bond lengths (Co1–P1 2.1874(6) Å, Co1–P2 2.1570(6) Å) and the respective sums of angles around the phosphorus atoms ($\sum_{P1}$: 328.5(2)°, $\sum_{P2}$: 337.8(2)°) are significantly different, presumably due to the interaction of the [K(18-c-6)(dme)]$^+$ counterion with the cyclohexyl moiety of one of the isonitrile ligands which leads to a deviation from the expected ideal C_2 symmetry of [*rac*-**6**]$^-$. Significant backbonding from the cobalt atom to π* orbitals of the isonitrile ligands can be deduced from the C≡N–C bond angles in the solid state which deviate significantly from 180° (C3–N1–C5: 153.6(2)°, C4–N2–C6: 153.3(2)°).

The structure of [*rac*-**7**]$^-$ shows an anagostic[61] interaction between H1 (part of an *ortho*-methyl group on the mesityl substituent attached to P1) and the cobalt atom (Co1···H1: 2.64 Å, Fig. 3). This leads to a rather large deviation from the expected C_2 symmetry, with the tBu$_2$C$_2$P$_2$ ring notably tilted away from H1. In addition, the two phosphorus atoms of the bis(phosphanido) ligand in [*rac*-**7**]$^-$ show distinctly different coordination environments. While the Co1–P1 bond length (2.2371(4) Å) and $\sum_{P1}$ (325.3(2)°) indicate a Co–P single bond and a trigonal pyramidal environment around P1, the respective data for P2 indicate a Co=P double bond and a trigonal planar environment (Co1–P2: 2.0871(5) Å, $\sum_{P2}$: 351.1(2)°). Both this increased bond order and the anagostic interaction with H1 can be attributed to the more electron-poor and hence electrophilic Co atom in [*rac*-**7**]$^-$ than in [*rac*-**1**]$^-$ or [*rac*-**6**]$^-$ (*vide infra* for further discussion of electronic structures). It should be noted, however, that these features do not appear to be retained in solution, as evidenced by ^{31}P{^{1}H} NMR spectra of isolated [K(18-c-6)][*rac*-**7**] (*vide supra*; see also the ESI, Fig. S28 and S29,† for variable-temperature studies) which show only a single resonance for the bis(phosphanido) ligand with a similar chemical shift to those observed for [K(18-c-6)(thf)][*rac*-**1**] and [K(18-c-6)(dme)][*rac*-**6**]. The Co–C, Co–P and P–C bond lengths within the Co(η^4-1,3-tBu$_2$C$_2$P$_2$) fragment of [*rac*-**7**]$^-$ are all similar to those found in related complexes such as [Cp‴Co(η^4-1,3-tBu$_2$C$_2$P$_2$)][62] and [K(18-c-6)(thf)$_2$][Co(η^4-1,3-tBu$_2$C$_2$P$_2$)$_2$].[33]

In the solid state, the cobalt atom in [*meso*-**8**]$^-$ adopts a distorted trigonal antiprismatic environment, similar to that found in the neutral complex [(triphos)Co(η^3-P$_3$)] (triphos = 1,1,1-tris(diphenylphosphinomethyl)ethane).[63] While the Co–P1 and Co–P3 bonds (to the mesityl-substituted P atoms of the triphospholanido ligand) are in the range of Co–P single bonds (2.136(2) and 2.141(2) Å), the Co–P2 bond length (to the central unsubstituted P atom of the triphospholanido ligand) is considerably larger (2.382(2) Å), suggesting a rather weak interaction. Within the Co(*cyclo*-P$_3$) fragment, the P–P bond lengths (2.142(3)–2.164(3) Å), as well as the Co–P bond lengths (2.267(2)–2.283(4) Å), are similar to those found in [nBu$_4$N][(PHDI)Co(η^3-P$_3$)(CN)][39] and [(TMC)$_2$P][Cp‴Co(η^3-P$_3$)].[40]

The dianion [*rac*-**9**]$^{2-}$ consists of two neutral [Co^{II}{1,2-(PMes)$_2$C$_2$B$_{10}$H$_{10}$}] fragments bridged by the *cis*-tetraphosphabutadienediide ligand. The dianion has a mirror plane formed by the planar P$_4^{2-}$ ligand. The phosphorus atoms within the bis(phosphanido) ligands are chemically inequivalent as indicated by their significantly different Co–P bond lengths (Co1–P1 2.246(2) Å, Co1–P2 2.170(2) Å) and sum of angles around the phosphorus atoms ($\sum_{P1}$: 323.5(8)°, $\sum_{P2}$ 340.7(7)°). The P–P bond lengths (2.095(3)–2.336(3) Å) as well as the Co–P bond lengths (2.183(2)–2.340(2) Å) within the Co$_2$P$_4$ fragment are comparable to those found in [K(dme)$_4$][{(BIAN)Co}$_2$(μ-η^4:η^4-P$_4$)].[28] In contrast, the Co–Co distance in [*rac*-**9**]$^{2-}$ (2.651(1) Å) is indicative of a Co–Co single bond and is notably shorter than in the aforementioned BIAN complex (2.8455(5) Å), although a similar metal–metal distance was found in [{Cp‴Fe}$_2$(μ-η^4:η^4-P$_4$)] (2.6430(8) Å).[47]

Quantum chemical and electronic structure analysis of *rac*-2 and complex anions [*rac*-**1**]$^-$, [*rac*-**6**]$^-$, [*rac*-**7**]$^-$, [*meso*-**8**]$^-$ and [*rac*-**9**]$^{2-}$

Cobalt complexes [K(18-c-6)(thf)][*rac*-**1**], [K(18-c-6)(dme)][*rac*-**6**], [K(18-c-6)][*rac*-**7**], [K(18-c-6)] [*meso*-**8**] and [K(18-c-6)]$_2$[*rac*-**9**] were further characterised by UV-vis spectroscopy in THF to provide experimental insight into their electronic structures. Gratifyingly, nickel complex *rac*-**2** was sufficiently soluble and stable in THF to allow for the measurement of UV-vis spectra as well (see the ESI, Fig. S39–S50†). To complement these experimental studies, TDDFT calculations at the ωB97X-D3/def2-TZVP CPCM(THF) level were also conducted, to give further insight into the relevant electronic transitions. As is typically observed for range-separated functionals, the calculated spectra are blue-shifted with respect to the experimental spectra.

Nevertheless, the overall shape of the spectra is very well reproduced (see the ESI, Fig. S39–S50†), and the calculated difference densities were thus used to assign the nature of the observed transitions. A summary of the UV-vis data is given in Table 1, and it can be seen that the spectra are dominated by charge-transfer transitions. It is noteworthy that [K(18-c-6)(thf)]

Table 1 Summary of UV-vis spectroscopic data. MLCT = metal-to-ligand charge-transfer, LMCT = ligand-to-metal charge-transfer

	λ_{max} [nm]	ε [10^3 L mol^{-1} cm^{-1}]	Transition type
[*rac*-**1**]$^-$	337, 435, 768	13.3, 6.2, 1.9	MLCT, LMCT, MLCT
rac-**2**	271, 340, 424, 527, 898	8.8, 9.7, 1.7, 1.9, 0.7	MLCT, MLCT, LMCT/d–d LMCT/d–d, d–d
[*rac*-**6**]$^-$	277, 342, 490, 655	11.6, 8.6, 3.4, 0.7	MLCT/n–π*, MLCT, MLCT, MLCT
[*rac*-**7**]$^-$	354, 404, 513, 810	11.5, 6.3, 4.3, 2.3	n–π*, LMCT, d–d, MLCT
[*meso*-**8**]$^-$	287, 337, 398	16.3, 18.3, 6.8	MLCT, MLCT, d–d/LMCT
[*rac*-**9**]$^{2-}$	357, 533	20.1, 14.4	n–π*, LMCT/n–π*

[*rac*-**1**], [K(18-c-6)(dme)][*rac*-**6**], and [K(18-c-6)][*rac*-**7**] share similar metal-to-ligand charge-transfer (MLCT) transitions from 3d electrons at cobalt into π* orbitals at their ligands as their lowest-energy transitions. Here, the wavelength λ_{max} of these transitions increases in the order [K(18-c-6)(dme)][*rac*-**6**] < [K(18-c-6)(thf)][*rac*-**1**] < [K(18-c-6)][*rac*-**7**], which neatly coincides with the order of the π-accepting abilities of the ligands in these complexes (*vide infra*), since more strongly accepting ligands require less energy for an MLCT transition.

CASSCF calculations were also performed for the cobaltate anions [*rac*-**1**]$^-$, [*rac*-**6**]$^-$, [*rac*-**7**]$^-$, [*meso*-**8**]$^-$ and the nickel complex *rac*-**2** to gain a deeper insight into their electronic structures. Due to its size and the presence of two metal centres, complex dianion [*rac*-**9**]$^{2-}$ was instead analysed by broken-symmetry DFT (BS-DFT) calculations. The CASSCF calculations for the complexes [*rac*-**1**]$^-$, *rac*-**2**, [*rac*-**6**]$^-$, [*rac*-**7**]$^-$ and [*meso*-**8**]$^-$ revealed only moderate multireference character (for depiction of the CASSCF orbitals, see the ESI, Fig. S51–S55†) with contributions of the ground-state configuration function to the overall electronic structure of between 85% ([*rac*-**7**]$^-$) and 88% ([*rac*-**6**]$^-$). As a result, DFT-based energy decomposition methods such as EDA-NOCV (energy decomposition analysis with natural orbitals of chemical valence)[64] could be used to quantify the interactions between the cobalt atom and the ligands in the cobalt complexes [*rac*-**1**]$^-$, [*rac*-**6**]$^-$, [*rac*-**7**]$^-$ and [*meso*-**8**]$^-$ (Table 2).

For the four cobalt complexes, the interactions between the metal centres and the ligands were found to be highly covalent in nature. Thus, assignments of oxidation states are somewhat ambiguous. Still, in the case of [*rac*-**1**]$^-$ and [*rac*-**6**]$^-$, the CASSCF calculations indicate the expected presence of a $3d^8$ Co^{I} atom coordinated by a σ-donating bis(phosphanido) ligand. Furthermore, the EDA-NOCV calculations show that the cod ligand in **1**$^-$ acts as a weakly σ-donating (29 kcal mol^{-1}) and strongly π-accepting (150 kcal mol^{-1}) ligand (see the ESI† and Table 1). As expected, the isonitrile ligands in [*rac*-**6**]$^-$ act as comparatively stronger σ-donating (52 kcal mol^{-1}) but weaker π-accepting (93 kcal mol^{-1}) ligands.

In contrast to [*rac*-**1**]$^-$ and [*rac*-**6**]$^-$, the oxidation state of the cobalt atom in [*rac*-**7**]$^-$ cannot be derived as straightforwardly from the CASSCF calculations. For example, one orbital pair describing the Co–((η^4-1,3-*t*Bu$_2$C$_2$P$_2$) π interactions is depicted in Fig. 4. Here, the bonding orbital (183) shows almost equal contributions from cobalt and the diphosphacyclobutadiene ligand (44% Co, 41% *t*Bu$_2$C$_2$P$_2$). Based on these data, the electronic structure of [*rac*-**7**]$^-$ can be described as intermediate between two extreme cases: a cobalt(III) complex with a strong π-donating diphosphacyclobutadienediide ligand (case i) or a cobalt(I) complex with a strong π-accepting diphosphacyclobutadiene ligand (case ii). The same ambiguity was also found previously for the homoleptic complex [K(18-c-6)(thf)$_2$][Co(η^4-1,3-*t*Bu$_2$C$_2$P$_2$)$_2$].[34] However, similarly to [*rac*-**1**]$^-$ and [*rac*-**6**]$^-$, [*rac*-**7**]$^-$ shows an MLCT band as the lowest absorption in its UV-vis spectrum (*vide supra*) which seems unlikely to occur in case i. Thus, the spectroscopic data suggest that the electronic structure of [*rac*-**7**]$^-$ is probably closer to case ii. For that case, EDA-NOCV calculations indeed show that the π-accepting properties of the *t*Bu$_2$C$_2$P$_2$ ligand dominate and account for 75% (160 kcal mol^{-1}) of the total interaction between the cobalt atom and the *t*Bu$_2$C$_2$P$_2$ ligand.

Analysis of the wave function of [*meso*-**8**]$^-$ obtained from the CASSCF calculation confirms σ-bonding interactions between Co1 and P2 (the central P atom of the triphospholanido ligand)

Table 2 Summary of EDA-NOCV calculations on complex anions [*rac*-**1**]$^-$, [*rac*-**6**]$^-$, [*rac*-**7**]$^-$, [*meso*-**8**]$^-$. All energies are given in kcal mol^{-1}. E_{int}: total interaction energy between the two given fragments. $E_{L\rightarrow M}$: interaction energy arising from donor interactions between the ligand fragment and the cobalt atom (a: σ–donor interactions, b: π–donor interactions). $E_{M\rightarrow L}$: interaction energy arising from π backdonation from the cobalt atom to the ligand fragment

	Fragments	E_{int}	$E_{L\rightarrow M}$	$E_{M\rightarrow L}$
[*rac*-**1**]$^-$	[Co{1,2-(PMes)$_2$C$_2$B$_{10}$H$_{10}$}]$^-$, cod	190	29^b	150
[*rac*-**6**]$^-$	[Co{1,2-(PMes)$_2$C$_2$B$_{10}$H$_{10}$}]$^-$, 2 CyNC	162	52^a	93
[*rac*-**7**]$^-$	[Co{1,2-(PMes)$_2$C$_2$B$_{10}$H$_{10}$}]$^-$, *t*Bu$_2$C$_2$P$_2$	214	28^b	161
[*meso*-**8**]$^-$	[Co{1,2-(P$_3$Mes$_2$)C$_2$B$_{10}$H$_{10}$}], P$_3^-$	175	66^b	82

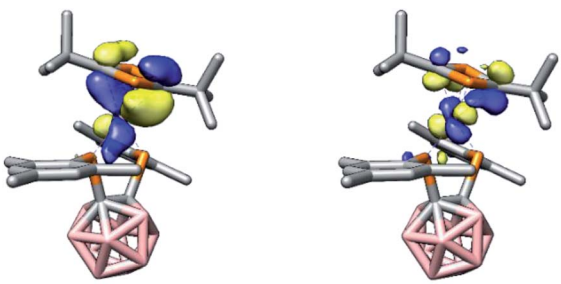

Fig. 4 CASSCF natural orbitals of [*rac*-**7**]$^-$ describing the π interaction between the cobalt atom and the η^4-1,3-*t*Bu$_2$C$_2$P$_2$ ligand (183: bonding; 184: antibonding). Orbital occupations and contributions of 3d orbitals on Co are given in parentheses. Surface isovalue = 0.05.

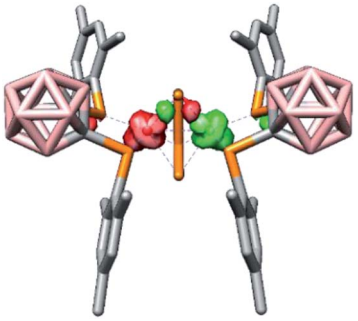

Fig. 5 Spin density plot of the dianion $[rac\text{-}\mathbf{9}]^{2-}$ obtained from a BS-DFT calculation.

despite the relatively long distance between these atoms observed crystallographically (*vide supra*; see the ESI† for full details). In addition, the CASSCF calculations show that the *cyclo*-P_3^- ligand functions as both a strong π donor and a strong π acceptor. These findings are supported by the EDA-NOCV calculations which show that π donation accounts for 38% and backdonation accounts for 47% of the total interaction between cobalt and the *cyclo*-P_3 ligand (Table 2).

For dianion $[rac\text{-}\mathbf{9}]^{2-}$, the BS-DFT calculations revealed that two low-spin $3d^7$ cobalt(II) atoms are antiferromagnetically coupled *via* P3 (one of the terminal P atoms of the P_4^{2-} chain, $J = -1837$ cm^{-1}; see Fig. 5 for a depiction of the spin density). The solution NMR data offer indirect proof of this antiferromagnetic coupling between the cobalt(II) atoms, since the calculated ^{31}P NMR shifts are only in reasonable agreement with the experimental data when a broken-symmetry wave function is utilised. In particular, the shift of P3 showed an exceptionally large deviation from the experimental data when a closed-shell singlet wave function was used (218 *vs.* 419 ppm, see the ESI†). Notably, no direct Co–Co bonds were found, but bonding interactions between the cobalt atoms do occur *via* three-centre two-electron bonds involving Co1, Co1′ and P3 or P6, respectively (see the ESI†). Furthermore, in agreement with classical electron-counting rules, the Co_2P_4 fragment in $[rac\text{-}\mathbf{9}]^{2-}$ contains 14 cluster electrons. Thus, $[rac\text{-}\mathbf{9}]^{2-}$ obeys the $2n + 2$ (n = number of cluster vertices) criterion to be classified as a *closo* cluster. The shape of the Co_2P_4 fragment – a distorted bicapped tetrahedron or capped trigonal bipyramid (Scheme 6) – differs from the octahedral shape predicted by the Wade–Mingos rules. However, such deviations are common, especially in mixed transition metal–main group element clusters.[65]

For nickel complex *rac*-**2**, the CASSCF calculations indicate the absence of π bonding between the bis(phosphanido) ligand and the $3d^8$ nickel(II) atom, thus supporting the conclusions drawn from the analysis of the solid-state molecular structure (see the ESI, Fig. S52†).

Redox properties of complexes [K(18-c-6)(thf)][*rac*-1], [K(18-c-6)(dme)][*rac*-6], [K(18-c-6)][*rac*-7], [K(18-c-6)][*meso*-8] and [K(18-c-6)]$_2$[*rac*-9]

The redox properties of the cobalt complexes were investigated by cyclic voltammetry (CV) in THF/[nBu$_4$N](PF$_6$). The results are summarised for a scan rate of 0.20 V s^{-1} in Table 3 (all referenced against FcH/FcH$^+$ (FcH = [Cp$_2$Fe])). All complexes show one oxidation event in the range of −1.50 to −0.10 V, with the exception of $[rac\text{-}\mathbf{9}]^{2-}$ which shows four oxidation events (see the ESI† for CV data of the complexes in a larger range). Cobalt complex $[rac\text{-}\mathbf{1}]^-$ shows a quasi-reversible oxidation at $E_{1/2} = -1.13$ V which is considerably higher than that observed in the related cobalt(I) complex [K(thf)$_2$][Co(BIAN)(cod)] ($E_{1/2} = -1.72$ V), presumably due to the strong inductive electron-withdrawing effect of the carborane backbone. When comparing the complexes $[rac\text{-}\mathbf{1}]^-$, $[rac\text{-}\mathbf{6}]^-$ and $[rac\text{-}\mathbf{7}]^-$, their oxidation potentials increase in the order $[rac\text{-}\mathbf{6}]^- < [rac\text{-}\mathbf{1}]^- < [rac\text{-}\mathbf{7}]^-$. This trend nicely follows the order of the π-accepting properties of the ligands in these complexes (isonitrile < cod < 1,3-diphosphacyclobutadiene, see Table 3). Among the cobalt complexes, $[meso\text{-}\mathbf{8}]^-$ is oxidised at the highest potential ($E = -0.79$ V). The bimetallic complex $[rac\text{-}\mathbf{9}]^{2-}$ shows a particularly rich redox chemistry. Here, an irreversible oxidation at $E = -0.97$ V is followed by three quasi-reversible oxidations at $E_{1/2} = -0.79$, −0.56 and −0.18 V.

Table 3 Summary of redox properties of [K(18-c-6)][*rac*-**1**], [K(18-c-6)(dme)][*rac*-**6**], [K(18-c-6)][*rac*-**7**], [K(18-c-6)][*meso*-**8**] and [K(18-c-6)]$_2$[*rac*-**9**]. A star (*) denotes an irreversible oxidation process and only the peak potential is given in that case

	$[rac\text{-}\mathbf{1}]^-$	$[rac\text{-}\mathbf{6}]^-$	$[rac\text{-}\mathbf{7}]^-$	$[meso\text{-}\mathbf{8}]^-$	$[rac\text{-}\mathbf{9}]^{2-}$
$E_{1/2}^{ox}$	−1.13	−1.48	−0.81	−0.79*	−0.97*, −0.79, −0.56, −0.18

Conclusions

Through rational ligand modification we have been able to prepare the first examples of heteroleptic transition metal complexes incorporating powerful electron-donating carborane-bridged bis(phosphanido) ligands. These complexes have been obtained through simple oxidation reactions of convenient, low-valent Co and Ni sources with a carborane-bridged diphosphetane. For the resulting Co complex [K(18-c-6)(thf)][*rac*-**1**] we have shown that the presence of a labile cod ligand allows for extensive further reactivity, which can be used to prepare various other bis(phosphanido)-containing products. These reactions include not only simple ligand substitutions, but also well-defined, inner-sphere small molecule aggregation and degradation. Particularly dramatically, the highly nucleophilic bis(phosphanido) ligand in [K(18-c-6)(thf)][*rac*-**1**] enables an unusual activation of white phosphorus to yield a remarkable triphospholanido complex [K(18-c-6)][*meso*-**8**], in an unprecedented inner-sphere fragmentation of the P_4 molecule into P^+ and P_3^- motifs, the latter resulting in a very rare *cyclo*-P_3^- ligand. The rather facile synthetic access to [K(18-c-6)][*meso*-**8**] renders this complex a promising candidate for further experimental studies with the aim of liberating and/or functionalising the *cyclo*-P_3^- fragment. These studies are ongoing in our laboratories.

Data availability

The data supporting the findings of this study are available within the paper and its ESI† files. Crystallographic have been deposited at the CCDC under 2086046 ([K(dme)$_4$][*rac*-**1**]), 2086047 (*rac*-**2**), 2086048 ([K(18-c-6)(dme)][*rac*-**6**]), 2086049 ([K(dme)$_4$][*rac*-**7**]), 2086050 [K(18-c-6)(dme)$_2$][*meso*-**8**] and 2086051 ([K(dme)][K(dme)$_2$][*rac*-**9**]).

Author contributions

E. H.-H., R. W. and P. C. conceived the project. P. C. performed the preparative experiments and theoretical investigations and analysed the data. J. L. recorded and analysed cyclic voltammograms und UV-vis spectra. G. H. contributed to the synthetic investigations. I. G. S recorded and analysed solid-state NMR spectra. P. C. and D. J. S. wrote the manuscript with input from R. W. and E. H.-H.

Conflicts of interest

There are no conflicts to declare.

Acknowledgements

We thank Karolina Trabitsch for experimental assistance. Financial support by the European Research Council (ERC CoG 772299) is gratefully acknowledged.

Notes and references

§ Reduction to generate product *rac*-**5** is significantly slower than the analogous reaction to generate the *tert*-butyl-substituted analogue investigated previously, which is consistent with the increased steric bulk of the mesityl groups.

¶ Similar to carbonyl ligands, the lowering of the CN-stretching vibration in isonitrile ligands is caused by the partial occupation of the respective π^* antibonding orbitals as a consequence of backbonding from the metal centre.

‖ We wish to note that *rac*-**5** does not react with P_4 in THF at room temperature according to ^{31}P NMR studies.

1 L. Rosenberg, *Coord. Chem. Rev.*, 2012, **256**, 606–626.
2 J. G. Planas and J. A. Gladysz, *Inorg. Chem.*, 2002, **41**, 6947–6949.
3 J. Giner Planas, F. Hampel and J. A. Gladysz, *Chem.–Eur. J.*, 2005, **11**, 1402–1416.
4 E. J. Derrah, D. A. Pantazis, R. McDonald and L. Rosenberg, *Organometallics*, 2007, **26**, 1473–1482.
5 P. Mastrorilli, *Eur. J. Inorg. Chem.*, 2008, 4835–4850.
6 R. Waterman, *Dalton Trans.*, 2009, 18–26.
7 V. Nesterov, G. Schnakenburg, A. Espinosa and R. Streubel, *Inorg. Chem.*, 2012, **51**, 12343–12349.
8 R. Waterman, *Chem. Soc. Rev.*, 2013, **42**, 5629–5641.
9 L. Rosenberg, *ACS Catal.*, 2013, **3**, 2845–2855.
10 Y. Gloaguen, W. Jacobs, B. de Bruin, M. Lutz and J. I. van der Vlugt, *Inorg. Chem.*, 2013, **52**, 1682–1684.
11 P. E. Sues, A. J. Lough and R. H. Morris, *J. Am. Chem. Soc.*, 2014, **136**, 4746–4760.
12 R. Waterman, D. J. Mindiola, C. R. Clough and G. L. Hillhouse, *Inorg. Chim. Acta*, 2014, **422**, 57–64.
13 A. M. Geer, Á. L. Serrano, B. de Bruin, M. A. Ciriano and C. Tejel, *Angew. Chem., Int. Ed.*, 2015, **54**, 472–475.
14 E. C. Y. Tam, D. C. Apperley, J. D. Smith, M. P. Coles and J. R. Fulton, *Inorg. Chem.*, 2017, **56**, 14831–14841.
15 D. Wang, Q. Chen, X. Leng and L. Deng, *Inorg. Chem.*, 2018, **57**, 15600–15609.
16 K. Kaniewska, A. Dragulescu-Andrasi, Ł. Ponikiewski, J. Pikies, S. A. Stoian and R. Grubba, *Eur. J. Inorg. Chem.*, 2018, 4298–4308.
17 A. Schmer, N. Volk, A. E. Ferao and R. Streubel, *Dalton Trans.*, 2018, **48**, 339–345.
18 V. Varela-Izquierdo, A. M. Geer, B. de Bruin, J. A. López, M. A. Ciriano and C. Tejel, *Chem.–Eur. J.*, 2019, **25**, 15915–15928.
19 J. Yang, S. Langis-Barsetti, H. C. Parkin, R. McDonald and L. Rosenberg, *Organometallics*, 2019, **38**, 3257–3266.
20 H. Köpf and V. Richtering, *J. Organomet. Chem.*, 1988, **346**, 355–360.
21 G. Sillett, L. Ricard, C. Patois and F. Mathey, *J. Am. Chem. Soc.*, 1992, **114**, 9453–9457.
22 A. Moores, N. Mézailles, L. Ricard, F. Mathey and P. L. Floch, *Chem. Commun.*, 2003, 1914–1915.
23 P. Coburger, S. Demeshko, C. Rödl, E. Hey-Hawkins and R. Wolf, *Angew. Chem., Int. Ed.*, 2017, **56**, 15871–15875.
24 K. Lee, C. E. Moore and C. M. Thomas, *Organometallics*, 2020, **39**, 2053–2056.
25 A. Kreienbrink, M. B. Sárosi, E. G. Rys, P. Lönnecke and E. Hey-Hawkins, *Angew. Chem., Int. Ed.*, 2011, **50**, 4701–4703.
26 F. Nief and F. Mathey, *Tetrahedron*, 1991, **47**, 6673–6680.
27 A. R. Popescu, F. Teixidor and C. Viñas, *Coord. Chem. Rev.*, 2014, **269**, 54–84.
28 S. Pelties, T. Maier, D. Herrmann, B. de Bruin, C. Rebreyend, S. Gärtner, I. G. Shenderovich and R. Wolf, *Chem.–Eur. J.*, 2017, **23**, 6094–6102.
29 P. Coburger, S. Demeshko, C. Rödl, E. Hey-Hawkins and R. Wolf, *Angew. Chem.*, 2017, **129**, 16087–16091.
30 I. Beaumont and A. H. Wright, *J. Organomet. Chem.*, 1992, **425**, C11–C14.
31 J. W. Dart, M. K. Lloyd, R. Mason, J. A. McCleverty and J. Williams, *J. Chem. Soc., Dalton Trans.*, 1973, 1747–1751.
32 C. A. L. Becker, M. A. Salam Biswas and J. C. Cooper, *Inorg. Chim. Acta*, 1991, **188**, 191–194.
33 R. Wolf, A. W. Ehlers, J. C. Slootweg, M. Lutz, D. Gudat, M. Hunger, A. L. Spek and K. Lammertsma, *Angew. Chem., Int. Ed.*, 2008, **47**, 4584–4587.
34 R. Wolf, A. W. Ehlers, M. M. Khusniyarov, F. Hartl, B. de Bruin, G. J. Long, F. Grandjean, F. M. Schappacher, R. Pöttgen, J. C. Slootweg, M. Lutz, A. L. Spek and K. Lammertsma, *Chem.–Eur. J.*, 2010, **16**, 14322–14334.
35 C. Rödl, K. Schwedtmann, J. J. Weigand and R. Wolf, *Chem.–Eur. J.*, 2019, **25**, 6180–6188.
36 M. Caporali, L. Gonsalvi, A. Rossin and M. Peruzzini, *Chem. Rev.*, 2010, **110**, 4178–4235.
37 C. M. Hoidn, D. J. Scott and R. Wolf, *Chem.–Eur. J.*, 2021, **27**, 1886–1902.

38 L. Giusti, V. R. Landaeta, M. Vanni, J. A. Kelly, R. Wolf and M. Caporali, *Coord. Chem. Rev.*, 2021, **441**, 213927.
39 C. M. Hoidn, T. M. Maier, K. Trabitsch, J. J. Weigand and R. Wolf, *Angew. Chem., Int. Ed.*, 2019, **58**, 18931–18936.
40 M. Piesch, S. Reichl, M. Seidl, G. Balázs and M. Scheer, *Angew. Chem., Int. Ed.*, 2019, **58**, 16563–16568.
41 M. Piesch, S. Reichl, M. Seidl, G. Balázs and M. Scheer, *Angew. Chem., Int. Ed.*, 2021, **60**, 15101–15108.
42 A. Kreienbrink, S. Heinicke, T. T. Duong Pham, R. Frank, P. Lönnecke and E. Hey-Hawkins, *Chem.–Eur. J.*, 2014, **20**, 1434–1439.
43 P. Coburger, H. Grützmacher and E. Hey-Hawkins, *Chem. Commun.*, 2019, **55**, 3187–3190.
44 M. Peruzzini, J. A. Ramirez and F. Vizza, *Angew. Chem., Int. Ed.*, 1998, **37**, 2255–2257.
45 S. Du, J. Yin, Y. Chi, L. Xu and W.-X. Zhang, *Angew. Chem., Int. Ed.*, 2017, **56**, 15886–15890.
46 R. Grünbauer, G. Balázs and M. Scheer, *Chem.–Eur. J.*, 2020, **26**, 11722–11726.
47 M. D. Walter, J. Grunenberg and P. S. White, *Chem. Sci.*, 2011, **2**, 2120–2130.
48 O. J. Scherer, T. Hilt and G. Wolmershäuser, *Organometallics*, 1998, **17**, 4110–4112.
49 A. L. Spek, *Acta Crystallogr., Sect. C: Struct. Chem.*, 2015, **71**, 9–18.
50 I. B. Sivaev, M. Y. Stogniy and V. I. Bregadze, *Coord. Chem. Rev.*, 2021, **436**, 213795.
51 D. M. Jenkins, T. A. Betley and J. C. Peters, *J. Am. Chem. Soc.*, 2002, **124**, 11238–11239.
52 D. M. Jenkins and J. C. Peters, *J. Am. Chem. Soc.*, 2005, **127**, 7148–7165.
53 R. G. Hayter, *J. Am. Chem. Soc.*, 1964, **86**, 823–828.
54 H. Werner, W. Hofmann, R. Zolk, L. F. Dahl, J. Kocal and A. Kühn, *J. Organomet. Chem.*, 1985, **289**, 173–188.
55 H.-F. Klein, M. Gaß, U. Zucha and B. Eisenmann, *Z. Naturforsch., B: J. Chem. Sci.*, 1988, **43**, 927–932.
56 B. Pan, M. W. Bezpalko, B. M. Foxman and C. M. Thomas, *Organometallics*, 2011, **30**, 5560–5563.
57 A. N. Kornev, V. V. Sushev, Y. S. Panova, N. V. Belina, O. V. Lukoyanova, G. K. Fukin, S. Y. Ketkov, G. A. Abakumov, P. Lönnecke and E. Hey-Hawkins, *Inorg. Chem.*, 2012, **51**, 874–881.
58 R. Beck and H.-F. Klein, *Acta Crystallogr., Sect. E: Struct. Rep. Online*, 2013, **69**, m604.
59 M. W. Bezpalko, A. M. Poitras, B. M. Foxman and C. M. Thomas, *Inorg. Chem.*, 2017, **56**, 503–510.
60 L. Yang, D. R. Powell and R. P. Houser, *Dalton Trans.*, 2007, 955–964.
61 M. Brookhart, M. L. H. Green and G. Parkin, *Proc. Natl. Acad. Sci. U. S. A.*, 2007, **104**, 6908–6914.
62 E.-M. Rummel, M. Eckhardt, M. Bodensteiner, E. V. Peresypkina, W. Kremer, C. Gröger and M. Scheer, *Eur. J. Inorg. Chem.*, 2014, 1625–1637.
63 M. Di Vaira, L. Sacconi and P. Stoppioni, *J. Organomet. Chem.*, 1983, **250**, 183–195.
64 M. P. Mitoraj, A. Michalak and T. Ziegler, *J. Chem. Theory Comput.*, 2009, **5**, 962–975.
65 F. Z. Trodi, G. Lucas, M. Bencharif, J.-F. Halet, S. Kahlal and J.-Y. Saillard, *J. Cluster Sci.*, 2007, **18**, 729–740.